Observational Study

Medicine®

OPEN

Integrative radiogenomic analysis for genomic signatures in glioblastomas presenting leptomeningeal dissemination

Hye Jin You (BS)[a], Ho-Young Park (MD)[b], Jinkuk Kim (PhD)[c,d,e], In-Hee Lee (PhD)[c,d,e], Ho Jun Seol (MD, PhD)[b], Jung-Il Lee (MD, PhD)[b], Sung Tae Kim (MD, PhD)[f], Doo-Sik Kong (MD, PhD)[a,b,*], Do-Hyun Nam (MD, PhD)[a,b,*]

Abstract

Despite therapeutic advances, the prognosis for glioblastoma (GBM) remains poor. In particular, leptomeningeal dissemination (LMD) has a dismal prognosis. The aim of this study was to identify tumor molecular phenotype, which has a great propensity to develop LMD. Between May 2004 and December 2012, a total of 145 GBM tumor samples were obtained from data registry. A total of 20 of the 145 patients with GBM were found to develop LMD. A specialized radiologist confirmed the diagnosis of LMD on magnetic resonance imaging. To clarify the genomic signatures in GBM with LMD, we performed integrative analysis of whole transcriptome sequencing and copy number alteration in the radiological features indicating LMD phenotypes in GBM. Eleven newly diagnosed patients with GBM with LMD had worse prognosis than those without LMD (median 5.55 vs. 12.94 months, $P < 0.0001$). Integrating analysis using gene expression based on the change of copy number revealed that SPOCK1, EHD2, SLC2A3, and ANXA11 were highly expressed with the gain of copy number, compared with the gene expression in the non-LMD group. In addition, it was demonstrated that NME2, TMEM100, and SIVA1 were downregulated with the loss of copy number. We also found that mesenchymal subtype accounted for 50% in LMD group, whereas mesenchymal subtype consisted of 29% in non-LMD group, even though there was no statistical significance ($P = 0.06$). Through this radiogenomic analysis, we suggested the possibility of finding candidate genes associated with LMD and highlighted the significance of integrating approach to clarify the molecular characteristics in LMD.

Abbreviations: CNA = copy number alteration, GBM = glioblastoma, indel = insertion/deletion, LMD = leptomeningeal dissemination, MR = magnetic resonance, WES = whole exome sequencing.

Keywords: glioblastoma, leptomeningeal dissemination, radiogenomic analysis

Editor: Yi Shu.

Funding: This research was supported by a grant of the Korea Health Technology R&D Project through the Korea Health Industry Development Institute (KHIDI), funded by the Ministry of Health & Welfare, Republic of Korea (HI14C3418), by the grant (NRF-2015M3A9A7029740, NRF-2015M3C9A1044522, and NRF-2015M3A9B5053642) of National Research Foundation funded by the Ministry of Science, ICT and Future Planning (MSIP) of Republic of Korea, by Samsung Medical Center grant, and by Samsung Biomedical Research Institute grant (SMX1161281).

Hye Jin You and Ho-Young Park contributed equally to this work.

The authors have no conflicts of interest to disclose.

Supplemental Digital Content is available for this article.

[a] Department of Health Sciences and Technology, SAIHST, Sungkyunkwan University, Seoul, Korea, [b] Departments of Neurosurgery, Samsung Medical Center, Sungkyunkwan University School of Medicine, Seoul, Korea, [c] Samsung Biomedical Research Institute, Samsung Medical Center, Seoul, Korea, [d] Institute for Refractory Cancer Research, Samsung Medical Center, Seoul, Korea, [e] Samsung Advanced Institute of Technology, Samsung Electronics Co. Ltd., Seoul, Korea, [f] Department of Radiology, Samsung Medical Center, Sungkyunkwan University School of Medicine, Seoul, Korea.

[*] Correspondence: Doo-Sik Kong, Sungkyunkwan University School of Medicine, Seoul, Republic of Korea (e-mail: neurokong@gmail.com, kds026@skku.edu); Do-Hyun Nam, Department of Neurosurgery, Samsung Medical Center, Sungkyunkwan University School of Medicine, Seoul, Republic of Korea (e-mail: biovioctory@gmail.com, nsnam@skku.edu).

Medicine (2016) 95:27(e4109)

Received: 13 October 2015 / Received in final form: 7 May 2016 / Accepted: 9 June 2016

http://dx.doi.org/10.1097/MD.0000000000004109

1. Introduction

Despite advances in surgical techniques, radiotherapy, and chemotherapy, glioblastoma (GBM) has still a poor prognosis. In particular, leptomeningeal dissemination (LMD) in the progression of GBM carries a worse prognosis. This condition has been considered a rare and serious condition, in which survival ranges from 12 to 20 weeks.[1–3] To date, only a few studies have reported an accurate incidence of LMD in GBM.[1,4] The overall incidence of LMD in GBM remains low. There have been potential risk components of LMD, specifically related to geographical location of the tumor or the proximity to the ventricular system. However, LMD can be sometimes found primarily in initial presentation as well as in the progressive stage of GBM regardless of communication with ventricle or subarachnoid cistern. Recent progress in the treatment of GBM has contributed to the prolongation of survival in GBM. This prolonged survival has led to the speculation that LMD has been reported with increasing frequency in recent years, occurring in up to 20% to 25% of newly diagnosed or recurrent GBM.[2,5–7] In addition, recent development of new molecular-targeting drugs is attributable to convert the tumor biology to a more invasive phenotype.[7–9] Mandel et al reported that increase in tumor invasiveness and predilection to disseminate into the cerebrospinal fluid (CSF), causing LMD, might be primarily related to molecular characteristics of the tumor.[7] To date, molecular signature associated with the development of LMD has not been identified. To address the hypothesis that GBM with LMD has worse prognosis and reflects underlying intertumoral molecular profiles, we performed integrative analysis of whole transcriptome sequencing (RNA-Seq) gene expression patterns, copy number alteration (CNA), and whole exome sequencing

Table 1

Characteristics of glioblastoma samples by status of LMD.

	LMD (20)	Non-LMD (125)
Median age, y	54	52
Newly diagnosed glioblastoma	11 (55%)	109 (87.2%)
Recurrent glioblastoma	9 (45%)	16 (12.8%)
Sex		
Male	8 (40%)	75 (60%)
Female	12 (60%)	50 (40%)
Molecular subtype		
Classical	3 (15%)	23 (18%)
Mesenchymal	10 (50%)	36 (29%)
Neural	2 (10%)	27 (21.8%)
Proneural	4 (20%)	32 (25.8%)
Unknown	1 (5%)	6 (4.8%)
Data availability		
RPKM	20 (100%)	124 (99.2%)
WES	17 (85%)	83 (66.4%)

LMD = leptomeningeal dissemination, non-LMD = nonleptomeningeal dissemination, RPKM = reads per kilobase per million mapped reads, WES = whole exome sequencing.

(WES) in the radiological features indicating LMD phenotypes in GBM.

2. Materials and methods

2.1. Patient sample preparation

Between May 2004 and December 2012, a total of 195 GBM tumor samples (145 patients) with available clinical and pathology reports were obtained from data registry in Samsung Medical Center (Seoul, Korea) because this group had the most extensive and complete follow-up data. All tissue samples had a pathologically confirmed diagnosis of GBM according to WHO criteria and collected with written informed consent under a protocol approved by the Institutional Review Board of the Samsung Medical Center (2010-04-004). All samples were from adult persons. Exclusion criteria included patients without histological confirmation of grade IV GBM and without agreement of this study. We identified 20 patients with GBM who developed LMD from our institutional database. The diagnosis of LMD was determined by radiographic findings on magnetic resonance (MR) imaging. Diagnostic lumbar puncture for CSF cytology was not performed, because the definition of LMD was not limited to the spinal arachnoid space, but to the intracranial dissemination. Data collected included demographic characteristics (age and sex), tumor characteristics (newly diagnosed or secondary GBM), survival from GBM diagnosis, time from GBM diagnosis to LMD diagnosis, and survival from the time of LMD diagnosis.[7] There were 120 newly diagnosed GBM and 25 recurrent setting of GBM. Patients consisted of 83 males and 62 females and the median age of the patients was 53 years (range, 16–80 years) (Table 1).

2.2. Definition of leptomeningeal dissemination on MR finding

The LMD was defined as positive findings in imaging evaluation of brain. All MRI exams were performed on a 1.5- or 3.0-T Signa Echospeed scanner (GE Medical Systems, Milwaukee, USA). To diagnose LMD, we set the radiographic criteria that were contrast enhancement of the leptomeninges around the outlines of the gyri and sulci or multiple nodular deposits in the subarachnoid space on T1 and/or T2 fluid attenuated inversion recovery gadolinium-enhanced MR images (Fig. 1). Imaging characteristics were established through a consensus of specialized neuroradiologists. All images were evaluated by consensus in a blinded fashion by 2 board-certified radiologists (S.T. Kim and J.H. Cha). Both readers were blinded to the genomic signatures and other clinical details at the time of image interpretation.

2.3. Genomic DNA and RNA isolation

DNA was isolated using the DNeasy kit (Qiagen, Hilden, Germany) according to the manufacturer's protocol. Total RNA was extracted from brain tumor tissue using the RNeasy kit (Qiagen, Hilden, Germany).

2.4. Survival analysis

Imaging and clinical follow-up were available for all patients. Patients were binary classified as presenting LMD or not on MR imaging as described earlier. The mainstay of survival analysis was the Cox proportional hazards model using R 3.0.1 (Vienna, Austria; http://www.R-project.org/) and P value <0.05 was deemed statistically significant. In order to assess the effects of a given predictor, we generally used the log-rank test.

2.5. Whole exome sequencing and copy number alteration

Capturing exonic DNA fragments was performed using either the Illumina TruSeq Exome-capture kit (for Case S780) or the Agilent SureSelect kit (for 100 other cases). Captured exonic DNA fragments were sequenced on the Illumina HiSeq2000 to generate 2×101 bp paired-end reads. BAM file was created by aligning paired-end WES reads using Burrows-Wheeler Aligner (version 0.6.2) to the human reference genome (hg 19). Sequences were sorted using SAMtools (version 0.1.18), and the duplicate reads were removed using Picard (version 1.73, http://picard.sourceforge.net). The predicted somatic mutations were annotated using Variant Effect Predictor (version 73).[10] When the matched normal WES data were not available, we used the mpileup command in SAMtools[11] with the preprocessed BAM files for tumor samples. The mpileup results were processed further to extract bases with a base quality of at least 15. To assemble a list of high-value mutations for initial validation, we selected all mutations meeting the following criteria: mutant allele read count ≥ 2, mutant allele fraction ≥ 0.01, and chromosomal coordinate of a mutation recorded as "confirmed somatic mutation" in COSMIC database (version 63).[12] Insertions/deletions (indels) were not called for tumors without the matched normal WES data. We used the patient-matched normal WES data to estimate the fold change in copy number in tumors. When the cases are not available to the patient-matched normal data, we made a "pseudo-normal" profile according to averaging a pool of 20 randomly chosen normal WES data, generated using the same sequencing platform and analysis pipeline as the tumor data. To do downstream analyses, including segmentation and calculation of the copy number for each gene, we used the ngCGH python package (version 0.4.4, http://github.com/seandavi/ngCGH), which is a tool for producing aCGH-like of next-generation sequencing data.

2.6. Whole transcriptome sequencing (RNA-Seq)

For each samples, we used the illumine TruSeq RNA Sample preparation kit to prepare RNA-Seq libraries. For analysis of mRNA level, we obtained the trimmed reads, which include 30

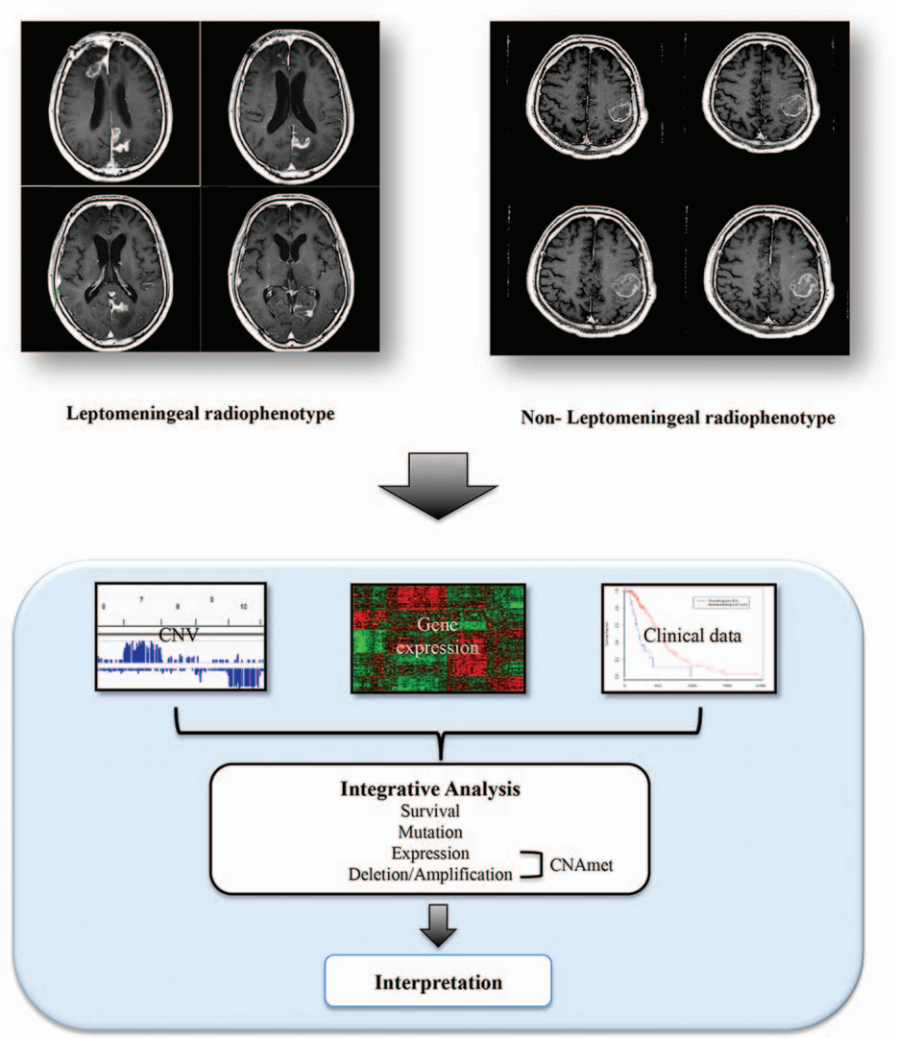

Figure 1. Schematic outline of this study.

nucleotides from the 5′ end of each read. The trimmed reads were aligned to the human reference genome (hg19) using GSNAP[13] (version 2012-12-20). We used R package DEGseq[14] to calculate gene expression as reads per kilobase per million mapped reads with RefSeq gene annotation ("refFlat" table downloaded from UCSC genome browser, last accessed on 2012/08/06).

2.7. Integration of copy number alteration and genome-wide expression analyses

RNA deep sequencing datasets were available in 144 of 145 patients and CNA datasets in 100 of 145 patients. Data from CNA and genome-wide expression profiles were analyzed individually. To identify the impact of CNA on gene expression, we utilize the following statistical approach. WES data were log-transformed. For each gene, the WES data were represented by a vector that was labeled 1 for amplification (log value >0) and 0 for no amplification. To identify the significant genes that exhibited CNA and gene expression changes, we modified an R package (CNAmet) that integrates high-throughput copy number data and expression data.[15] CNAmet algorithm followed next step. First, the signal-to-noise ratio statistic was used to link gene expression values to CNAs[16]:

$$W_i = \frac{m_1 - m_0}{\sigma_0 + \sigma_1}$$

where m_0 and σ_0, and m_1 and σ_1 represent the sample means and sample standard deviations for the expression level for non-amplified and amplified samples, respectively. Second, the weight values were combined to a score that indicated genes whose expression alterations were attributed to changes in copy number levels. If the difference of means of the groups is bigger and standard deviations within the groups are small, signal-to-noise statistics results in a large weight. Finally, we calculated corrected α values with a permutation test. We used permutation test in order to attain statistical significance. We conducted 10,000 permutations and got an α value. A low α value represents a close association between gene expression and gene amplification.

3. Results

3.1. GBM with LMD has worse clinical outcome than GBM without LMD

A total of 20 patients out of the 145 patients were identified to have developed LMD, yielding a rate of 13.8% of patients for this

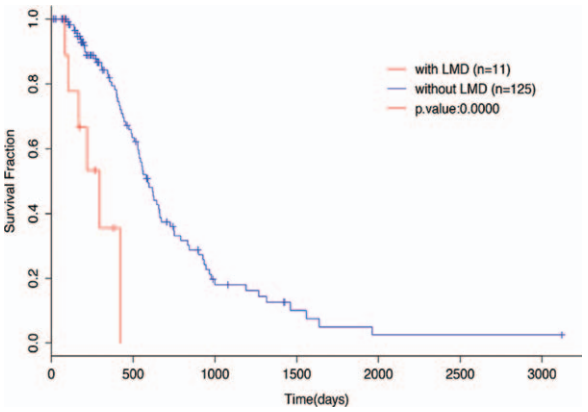

Figure 2. Kaplan–Meier analysis of overall survival between newly diagnosed patients with glioblastoma with and without LMD. *P* values are according to the log-rank test. LMD = leptomeningeal dissemination.

group. Eleven patients showed LMD in newly diagnosed GBM and 9 other patients showed LMD in the recurrent GBM (Table 1). Newly diagnosed tumor location was predominantly supratentorial (17 of 20 cases, 85%) and the remainder (3 cases) were infratentorial lesions. We analyzed the possible clinical factors to assess whether or not they affected LMD. The median follow-up period was 356 days. During the follow-up period, 5 of 20 patients with LMD survived, and 52 of 125 patients without LMD survived. In a total of 145 patients, median survival from the diagnosis as GBM was 12.3 months. In 20 patients with LMD, the interval between diagnosis of GBM and the occurrence of LMD ranged from 0 to 1442 days (mean, 214.85 days). Excluding the recurrent GBM in LMD group, from the diagnosis of GBM, overall survival analysis revealed that newly diagnosed patients with GBM with LMD (11 patients) had worse prognosis than those without LMD (median 5.55 vs. 12.94 months, $P < 0.0001$) (Fig. 2). Other clinical parameters such as age, performance status, and extent of resection were not significantly different between the groups (Table 1) (S1 Fig., http://links.lww.com/MD/B86).

3.2. Integrative approach for identification of differentially expressed genes

Compared to single type–based approach (gene expression or CNA), this proposed integrative approach (CNAmet) yielded a considerably smaller number and fewer portions of such synergistically impacted genes. As a result, it provided prevention from overestimation of candidate genes and a large number of genes fell into the class impacted definitely by only 1 genomic type under our integrative framework. As a result of integrating analysis using gene expression based on the change of copy number, we found that SPOCK1, SLC6A6, ODZ3, EHD2, EFNA5, SLC2A3, KIF3C, ANXA11, STK10, and C10orf90 were highly expressed with the gain of copy number, compared with the gene expression in the non-LMD group. In addition, it was demonstrated that GUK1, FAM195B, NUBP2, ROMO1, NME2, ANAPC11, TMEM100, RPL39L, NUDFB7, and SIVA1 were downregulated with the loss of copy number (Fig. 3A). The gene list can be found in Table 2. We performed GO and KEGG pathway analysis using Expression2Kinase software (http://www.maayanlab.net/X2K).[17] By importing the complete list of upregulated genes in LMD or non-LMD into the KEGG pathway and GO categories, we found that highly expressed genes in the LMD group were related to membrane part such as "anchored to plasma membrane (GO:0046658)" and "HSA04360_AXON_GUIDANCE" (Supplemental Table 1A, http://links.lww.com/MD/B86). Also we found that highly expressed genes in the non-LMD group were related to ubiquitination such as "HSA04120_UBIQUITIN_MEDIATED_PROTEOLYSIS" and "NADH dehydrogenase (ubiquinone) activity (GO:0008137)" (Supplemental Table 1B, http://links.lww.com/MD/B86).

3.3. Molecular subtypes in GBM with leptomeningeal dissemination

Recently, GBM populations have been clustered into 5 molecular subtypes (proneural, neural, classical, mesenchymal, and unknown) based on gene expression profiles.[18,19] We found that mesenchymal subtype accounted for 50% in LMD group, whereas mesenchymal subtype consisted of 29% in non-LMD group (Table 1). There was an increasing trend toward significance in the mesenchymal subtypes in LMD group, although there was no statistical significance ($P = 0.06$). We mapped the above-mentioned reference genes onto the 5 molecular subgroups defined by the TCGA network in non-LMD group (S2 Fig., http://links.lww.com/MD/B86).

3.4. Somatic mutation and copy number alteration in LMD group

Approach for GBM-related somatic mutation and CNA was to identify the characteristics of LMD group. There was no significant difference between patients with GBM with LMD and those without LMD in CNA (Fig. 3B). In detail, we found PTEN deletion (50%), EGFR amplification (35%), CDKN2A/B deletion (40%), CDK6 amplification (30%), MET amplification (30%), and RB1 deletion (15%) in 20 LMD samples (Fig. 4). Sixteen of 20 samples had available indel information, whereas 4 LMD samples were not available due to the matched normal pairs. PTEN, TP53, ATRX, and NF1 indel were very rare in LMD group. No IDH1 mutation (R132H) was found in the LMD group, compared with the incidence of 6 of 125 in the non-LMD group. We also found that only a few samples harbored EGFR mutation (A289V) (1 LMD and 4 non-LMD samples). Accordingly, there were no significant somatic mutations in the LMD group.

4. Discussion

Understanding the mechanism of leptomeningeal spreading and identification of genomic data leading to LMD is very critical to prolong the survival in patients with GBM. Distant metastasis of intracranial GBM such as LMD or spinal cord metastasis has been described with increasing frequency in recent years because of higher survival rates and prolonged survival times.[4] To date, the risk factors associated with LMD are not clearly understood.[2,20] Although some studies have demonstrated that communication with ventricular system is a critical factor for LMD in patients with malignant gliomas,[20–22] other studies reported that the proximity of tumor margin to ventricular system was not a risk factor for CSF dissemination.[4,23] This study revealed no significant association between ventricular opening and LMD, because adjacent cortical spread of LMD as well as distant leptomeningeal seeding around the brainstem or

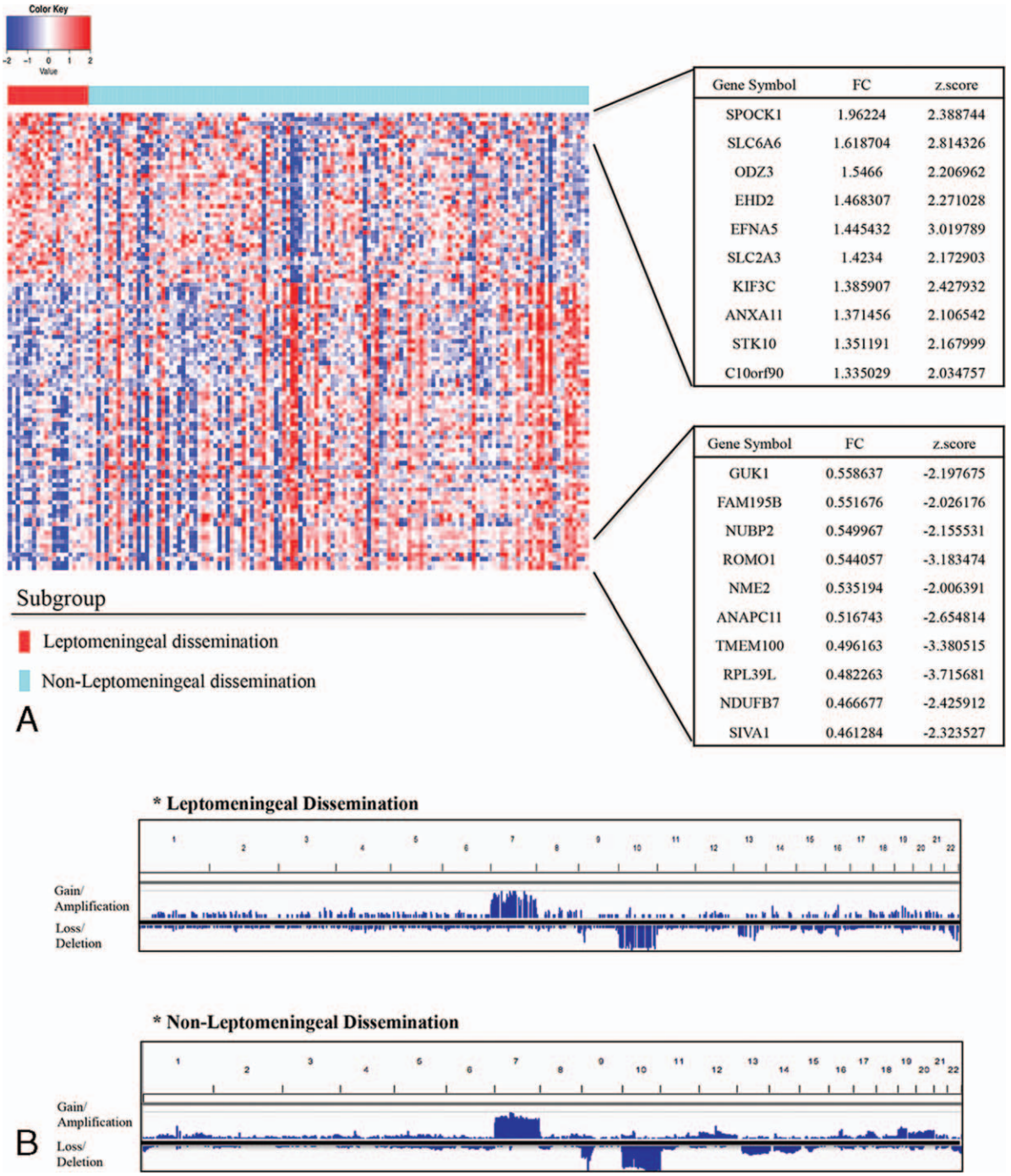

Gene Symbol	FC	z.score
SPOCK1	1.96224	2.388744
SLC6A6	1.618704	2.814326
ODZ3	1.5466	2.206962
EHD2	1.468307	2.271028
EFNA5	1.445432	3.019789
SLC2A3	1.4234	2.172903
KIF3C	1.385907	2.427932
ANXA11	1.371456	2.106542
STK10	1.351191	2.167999
C10orf90	1.335029	2.034757

Gene Symbol	FC	z.score
GUK1	0.558637	-2.197675
FAM195B	0.551676	-2.026176
NUBP2	0.549967	-2.155531
ROMO1	0.544057	-3.183474
NME2	0.535194	-2.006391
ANAPC11	0.516743	-2.654814
TMEM100	0.496163	-3.380515
RPL39L	0.482263	-3.715681
NDUFB7	0.466677	-2.425912
SIVA1	0.461284	-2.323527

Figure 3. Gene expression and CNA across LMD status. (A) Heat map demonstrating supervised hierarchical clustering of gene expression based on the change of CNA between patients with glioblastoma with and without LMD. Gene list defined using fold change cutoff (≥1.2 or ≤0.7) and *P*-value cutoff (<0.05). Top 10 genes and bottom 10 genes are represented with fold change, *z*-score. Red to blue color scale indicates the range from the highest positive to the highest negative correlation. (B) The distribution of CNA delineates amplification/deletion status in LMD and non-LMD. Chromosomes 1 to 22 are represented from left to right. Y-axis shows the relative number of patients according to status. Amplification means CNA ≥2.8 copy and deletion means CNA ≤1.4 copy. CNA = copy number alteration, LMD = leptomeningeal dissemination.

ventricular system was included in this study. The outcome of LMD in this study was compatible with the poor prognosis of patients with GBM with LMD as previously described.[2] Similarly, GBM with LMD at the initial presentation had a worse prognosis to newly diagnosed GBM without LMD in this study (Fig. 2). It still remains controversial whether the prognosis in patients with GBM with primarily presented LMD is poor or not.[24] In an attempt to clarify the risk factors for LMD, we investigated the molecular features in GBM with LMD in this study.

In the recent literature, there has been a little information about molecular characteristics in the LMD. Korshunov et al showed

Table 2

Description of 104 differentially expressed genes list integrating the change of copy number variation.

Gene	Description	FC	*z*-Score	*P*	*q*
SPOCK1	Sparc/osteonectin, cwcv and kazal-like domains proteoglycan (testican) 1	1.96224	2.3887	0.0169	0.0298
SLC6A6	Solute carrier family 6 (neurotransmitter transporter), member 6	1.618704	2.8143	0.0049	0.0159
ODZ3	TNM3 (teneurin transmembrane protein 3)	1.5466	2.2070	0.0273	0.0378
EHD2	EH-domain containing 2	1.468307	2.2710	0.0231	0.0363
EFNA5	Ephrin-A5	1.445432	3.0198	0.0025	0.0105
SLC2A3	Solute carrier family 2 (facilitated glucose transporter), member 3	1.4234	2.1729	0.0298	0.0378
KIF3C	Kinesin family member 3C	1.385907	2.4279	0.0152	0.0281
ANXA11	Annexin A11	1.371456	2.1065	0.0352	0.0406
STK10	Serine/threonine kinase 10	1.351191	2.1680	0.0302	0.0378
C10orf90	Chromosome 10 open reading frame 90	1.335029	2.0348	0.0419	0.0456
IQSEC1	IQ motif and Sec7 domain 1	1.329874	2.2299	0.0258	0.0377
C6orf106	Chromosome 6 open reading frame 106	1.326403	3.2810	0.0010	0.0063
GYS1	Glycogen synthase 1 (muscle)	1.321175	2.3417	0.0192	0.0327
ATP6AP1	ATPase, H^+ transporting, lysosomal accessory protein 1	1.308884	2.6954	0.0070	0.0191
NEDD4L	Neural precursor cell expressed, developmentally downregulated 4-like, E3 ubiquitin protein ligase	1.300947	2.1827	0.0291	0.0378
LARP1	La ribonucleoprotein domain family, member 1	1.292573	2.9824	0.0029	0.0110
SLIT3	Slit homolog 3 (*Drosophila*)	1.286466	2.1274	0.0334	0.0394
VPS18	Vacuolar protein sorting 18 homolog (*S cerevisiae*)	1.28096	2.9549	0.0031	0.0112
FLNB	Filamin B, beta	1.27831	2.0942	0.0362	0.0414
GDPD5	Glycerophosphodiester phosphodiesterase domain containing 5	1.277467	2.2222	0.0263	0.0378
ACSS2	Acyl-CoA synthetase short-chain family member 2	1.270948	2.5293	0.0114	0.0233
SLC36A1	Solute carrier family 36 (proton/amino acid symporter), member 1	1.257146	2.0349	0.0419	0.0456
RING1	Ring finger protein 1	1.254537	2.5667	0.0103	0.0227
GM2A	GM2 ganglioside activator	1.251046	2.1233	0.0337	0.0394
TM9SF4	Transmembrane 9 superfamily protein member 4	1.243239	2.5431	0.0110	0.0229
CNPY3	Canopy FGF signaling regulator 3	1.239517	2.7612	0.0058	0.0176
TNIP1	TNFAIP3 interacting protein 1	1.23667	2.5466	0.0109	0.0229
SLC29A3	Solute carrier family 29 (equilibrative nucleoside transporter), member 3	1.236227	2.0047	0.0450	0.0463
WDR37	WD repeat domain 37	1.233695	2.7470	0.0060	0.0177
HIF1AN	Transforming, acidic coiled-coil containing protein 1	1.23216	2.3110	0.0208	0.0339
ZNFX1	Zinc finger, NFX1-type containing 1	1.231896	2.2120	0.0270	0.0378
GTPBP2	GTP binding protein 2	1.227428	2.1534	0.0313	0.0383
CHP1	Calcineurin-like EF-hand protein 1	1.222177	2.4647	0.0137	0.0264
MFSD5	Major facilitator superfamily domain containing 5	1.221801	2.2432	0.0249	0.0375
GOLT1A	Golgi transport 1A	1.213351	2.0328	0.0421	0.0456
SUPT5H	Suppressor of Ty 5 homolog (*S cerevisiae*)	1.212656	2.0057	0.0449	0.0463
DOCK1	Dedicator of cytokinesis 1	1.212304	1.9668	0.0492	0.0492
PSEN2	Presenilin 2	1.204659	2.6127	0.0090	0.0203
TCTEX1D2	Tctex1 domain containing 2	0.699494	−3.8980	0.0001	0.0021
PSMA7	Proteasome (prosome, macropain) subunit, alpha type, 7	0.696636	−3.8872	0.0001	0.0021
MRPL36	Mitochondrial ribosomal protein L36	0.696227	−3.5782	0.0003	0.0033
NHP2	NHP2 ribonucleoprotein	0.693311	−2.9723	0.0030	0.0110
RBM3	RNA binding motif (RNP1, RRM) protein 3	0.692853	−2.7364	0.0062	0.0177
COL28A1	Collagen, type XXVIII, alpha 1	0.689611	−2.1405	0.0323	0.0386
PXMP2	Peroxisomal membrane protein 2	0.685728	−2.6511	0.0080	0.0194
NDUFB6	NADH dehydrogenase (ubiquinone) 1 beta subcomplex, 6	0.684164	−3.8470	0.0001	0.0021
FAM96A	Family with sequence similarity 96, member A	0.684025	−2.8405	0.0045	0.0156
MRPS12	Mitochondrial ribosomal protein S12	0.683946	−3.0963	0.0020	0.0090
C14orf142	Chromosome 14 open reading frame 142	0.683612	−3.6087	0.0003	0.0032
GINS2	GINS complex subunit 2 (Psf2 homolog)	0.683054	−2.0108	0.0443	0.0463
TRMU	TRNA 5-methylaminomethyl-2-thiouridylate methyltransferase	0.681434	−3.2337	0.0012	0.0067
ABRACL	ABRA C-terminal like	0.679872	−2.4876	0.0129	0.0252
RCN2	Reticulocalbin 2, EF-hand calcium-binding domain	0.677693	−2.6420	0.0082	0.0195
PRDX4	Peroxiredoxin 4	0.676417	−2.5043	0.0123	0.0245
TWF1	Twinfilin actin-binding protein 1	0.675474	−3.3089	0.0009	0.0063
GGH	Gamma-glutamyl hydrolase (conjugase, folylpolygammaglutamyl hydrolase)	0.674952	−2.6663	0.0077	0.0194
SRP9	Signal recognition particle 9 kDa	0.674681	−3.7852	0.0002	0.0023
TCEB2	Transcription elongation factor B (SIII), polypeptide 2 (18 kDa, elongin B)	0.672439	−4.0598	0.0000	0.0021
RPL35	Ribosomal protein L35	0.672265	−2.4032	0.0163	0.0291
NDUFA6	NADH dehydrogenase (ubiquinone) 1 alpha subcomplex, 6, 14 kDa	0.671061	−3.6662	0.0002	0.0028
GBAS	Glioblastoma amplified sequence	0.669219	−2.7314	0.0063	0.0177
PSPH	Phosphoserine Phosphatase	0.668928	−2.9769	0.0029	0.0110

(*continued*)

Table 2
(continued).

Gene	Description	FC	*z*-Score	*P*	*q*
COX6A1	Cytochrome C oxidase subunit VIa polypeptide 1	0.667729	−3.0929	0.0020	0.0090
ESCO2	Establishment of sister chromatid cohesion *N*-acetyltransferase 2	0.666113	−2.8294	0.0047	0.0156
EXOSC5	Exosome component 5	0.665005	−2.2952	0.0217	0.0348
GADD45GIP1	Growth arrest and DNA-damage-inducible, gamma interacting protein 1	0.660493	−2.1825	0.0291	0.0378
UQCR11	Ubiquinol-cytochrome C reductase, complex III subunit XI	0.655471	−3.0321	0.0024	0.0105
MRPL55	Mitochondrial ribosomal protein L55	0.6548	−2.1913	0.0284	0.0378
POLR2F	Polymerase (RNA) II (DNA directed) polypeptide F	0.653332	−3.2580	0.0011	0.0065
UBE2T	Ubiquitin-conjugating enzyme E2T	0.649707	−2.1698	0.0300	0.0378
PAM16	Presequence translocase-associated motor 16 homolog (*S cerevisiae*)	0.647954	−2.7810	0.0054	0.0171
MPST	Mercaptopyruvate sulfurtransferase	0.646581	−2.5529	0.0107	0.0229
E2F5	E2F transcription factor 5, P130-binding	0.644904	−3.2833	0.0010	0.0063
CHCHD2	Coiled-coil-helix-coiled-coil-helix domain containing 2	0.641235	−3.3404	0.0008	0.0062
LSM7	LSM7 homolog, U6 small nuclear RNA associated (*S cerevisiae*)	0.639373	−2.6885	0.0072	0.0191
ORC6	Origin recognition complex, subunit 6	0.632665	−3.1458	0.0017	0.0082
OXLD1	Oxidoreductase-like domain containing 1	0.627154	−1.9877	0.0468	0.0478
FAM195A	Family with sequence similarity 195, member A	0.624907	−1.9721	0.0486	0.0491
NDUFA11	NADH dehydrogenase (ubiquinone) 1 alpha subcomplex, 11, 14.7 kDa	0.620616	−2.4228	0.0154	0.0281
BIRC5	Baculoviral IAP repeat containing 5	0.615308	−2.0418	0.0412	0.0456
CDKN2A	Cyclin-dependent kinase inhibitor 2A	0.614364	−2.0395	0.0414	0.0456
BCL7C	B-cell CLL/lymphoma 7C	0.614273	−2.6332	0.0085	0.0195
HES4	Hes family BHLH transcription factor 4	0.607029	−2.2506	0.0244	0.0373
XRCC6BP1	XRCC6 binding protein 1	0.605205	−3.8604	0.0001	0.0021
C19orf25	Chromosome 19 open reading frame 25	0.6022	−2.3125	0.0207	0.0339
LYPLA1	Lysophospholipase I	0.599904	−3.5031	0.0005	0.0040
SCAND1	SCAN domain containing 1	0.598131	−2.1427	0.0321	0.0386
ECI1	Enoyl-CoA delta isomerase 1	0.595272	−2.2381	0.0252	0.0375
CRISPLD1	Cysteine-rich secretory protein LCCL domain containing 1	0.593685	−2.2141	0.0268	0.0378
LSMD1	*N* (alpha)-acetyltransferase 38, NatC auxiliary subunit	0.592943	−2.6721	0.0075	0.0194
C7orf50	Chromosome 7 open reading frame 50	0.578781	−2.3434	0.0191	0.0327
GADD45G	Growth arrest and DNA-damage-inducible, gamma	0.577906	−2.2675	0.0234	0.0363
CENPM	Centromere protein M	0.575361	−4.0565	0.0001	0.0021
PBK	PDZ binding kinase	0.569814	−2.1903	0.0285	0.0378
GUK1	Guanylate kinase 1	0.558637	−2.1977	0.0280	0.0378
FAM195B	Family with sequence similarity 195, member B	0.551676	−2.0262	0.0427	0.0458
NUBP2	Nucleotide binding protein 2	0.549967	−2.1555	0.0311	0.0383
ROMO1	Reactive oxygen species modulator 1	0.544057	−3.1835	0.0015	0.0076
NME2	NME/NM23 nucleoside diphosphate kinase 2	0.535194	−2.0064	0.0448	0.0463
ANAPC11	Anaphase promoting complex subunit 11	0.516743	−2.6548	0.0079	0.0194
TMEM100	Transmembrane protein 100	0.496163	−3.3805	0.0007	0.0058
RPL39L	Ribosomal protein L39-Like	0.482263	−3.7157	0.0002	0.0026
NDUFB7	NADH dehydrogenase (ubiquinone) 1 beta subcomplex, 7, 18 kDa	0.466677	−2.4259	0.0153	0.0281
SIVA1	SIVA1, apoptosis-inducing factor	0.461284	−2.3235	0.0202	0.0338

that gains of the 1p36 locus were closely related to symptomatic LMD of supratentorial GBM.[24] Another study suggested that mutations of the PTEN gene and a high MIB-1 labeling index were correlated with LMD in GBM.[25] In this study, we found that some genes were highly expressed in the LMD group based on the CNA change. As representative genes among them, SPOCK1 can activate PI3K/Akt signaling to block apoptosis and promote proliferation and metastasis in vitro and in vivo.[26] It is also known as a novel metastasis-related biomarker in lung cancer[27] and promotes hepatocellular carcinoma regulated by CHD1L.[28] EHD2, EH-domain containing 2, has a role of migration and invasion in the breast cancer cells.[29] As another candidate gene associated with LMD, ANXA11 and SLC2A3 are known to play a role of cellular invasion and metastasis in laryngeal cancer and hepatic carcinoma.[30,31] In particular, the mutation and deregulation of ANXA11 was reported to enhance cancer metastasis, invasion, and drug resistance through the platelet-derived growth factor receptor pathway and the mitogen-activated protein kinase/P53 pathway.[32] Among the downregulated genes in LMD group, NME2, TMEM100, and SIVA1 can be candidate genes promoting non-LMD. NME2 is known to reduce proliferation, migration, and invasion of gastric cancer cells to limit metastasis.[33]

We acknowledge that this study has some limitations such as relatively small sample size to draw a definite conclusion. In addition, the diagnosis of LMD in this study did not include cytological confirmation. In this study, the diagnosis of LMD was entirely based on the recent advances of radiological MR techniques, because CSF study has low sensitivity of the diagnosis of intracranial LMD, despite a higher specificity. Despite these limitations, we presented a trend of transcriptomic characterization between LMD and non-LMD cohorts based on genomic profiles for suggestive candidate genes associated with LMD prognosis.

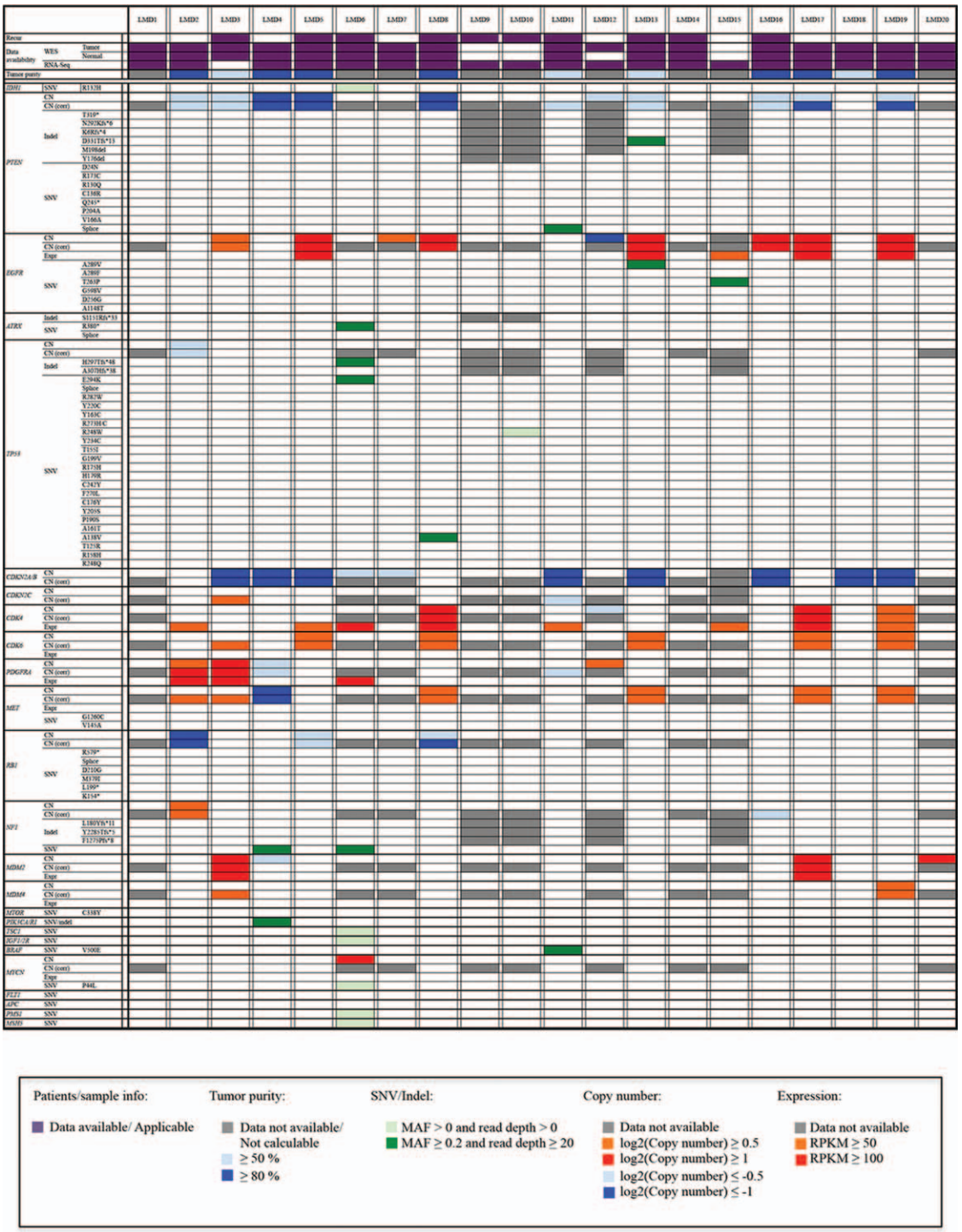

Figure 4. Key gene driver alterations in patients with glioblastoma with LMD. The 16 cases have WES data available for both the tumor and the paired normal tissues. WES has enabled detection of point mutations and indels (MAF ≥0.2 and read depth ≥20) and copy number changes (≥0.5 or ≤−0.5, log2 scale). CN = copy number, CN (corr) = corrected copy number, Expr = expression (mRNA), indel = insertion/deletion, LMD = leptomeningeal dissemination, MAF = mutant allele fraction, RPKM = read per kilobase per million, SNV = single nucleotide variant, WES = whole exome sequencing.

Through this radiogenomic analysis integrating gene expression, CNA, and mutation analysis, we suggested the possibility of finding candidate genes associated with LMD and highlighted the significance of integrating approach to clarify the molecular characteristics in LMD. To prove several candidate genes associated with LMD, we believe that further molecular experimental studies should be investigated in the future.

References

[1] Hamza MA, Mandel JJ, Conrad CA, et al. Survival outcome of early versus delayed bevacizumab treatment in patients with recurrent glioblastoma. J Neurooncol 2014;119:135–40.

[2] Arita N, Taneda M, Hayakawa T. Leptomeningeal dissemination of malignant gliomas. Incidence, diagnosis and outcome. Acta Neurochir (Wien) 1994;126:84–92.

[3] Chamberlain MC. Combined-modality treatment of leptomeningeal gliomatosis. Neurosurgery 2003;52:324–9. [discussion 330].
[4] Noh JH, Lee MH, Kim WS, et al. Optimal treatment of leptomeningeal spread in glioblastoma: analysis of risk factors and outcome. Acta Neurochir (Wien) 2015;157:569–76.
[5] Onda K, Tanaka R, Takahashi H, et al. Cerebral glioblastoma with cerebrospinal fluid dissemination: a clinicopathological study of 14 cases examined by complete autopsy. Neurosurgery 1989;25:533–40.
[6] Hubner F, Braun V, Richter HP. Case reports of symptomatic metastases in four patients with primary intracranial gliomas. Acta Neurochir (Wien) 2001;143:25–9.
[7] Mandel JJ, Yust-Katz S, Cachia D, et al. Leptomeningeal dissemination in glioblastoma; an inspection of risk factors, treatment, and outcomes at a single institution. J Neurooncol 2014;120:597–605.
[8] de Groot JF, Fuller G, Kumar AJ, et al. Tumor invasion after treatment of glioblastoma with bevacizumab: radiographic and pathologic correlation in humans and mice. Neuro Oncol 2010;12:233–42.
[9] Lu KV, Chang JP, Parachoniak CA, et al. VEGF inhibits tumor cell invasion and mesenchymal transition through a MET/VEGFR2 complex. Cancer Cell 2012;22:21–35.
[10] McLaren W, Pritchard B, Rios D, et al. Deriving the consequences of genomic variants with the Ensembl API and SNP Effect Predictor. Bioinformatics 2010;26:2069–70.
[11] Li H, Handsaker B, Wysoker A, et al. The Sequence Alignment/Map format and SAMtools. Bioinformatics 2009;25:2078–9.
[12] Forbes SA, Bindal N, Bamford S, et al. COSMIC: mining complete cancer genomes in the Catalogue of Somatic Mutations in Cancer. Nucleic Acids Res 2011;39:D945–950.
[13] Wu TD, Nacu S. Fast and SNP-tolerant detection of complex variants and splicing in short reads. Bioinformatics 2010;26:873–81.
[14] Wang L, Feng Z, Wang X, et al. DEGseq: an R package for identifying differentially expressed genes from RNA-seq data. Bioinformatics 2010;26:136–8.
[15] Louhimo R, Hautaniemi S. CNAmet: an R package for integrating copy number, methylation and expression data. Bioinformatics 2011;27:887–8.
[16] Golub TR, Slonim DK, Tamayo P, et al. Molecular classification of cancer: class discovery and class prediction by gene expression monitoring. Science 1999;286:531–7.
[17] Chen EY, Xu H, Gordonov S, et al. Expression2Kinases: mRNA profiling linked to multiple upstream regulatory layers. Bioinformatics 2012;28:105–11.
[18] Phillips HS, Kharbanda S, Chen R, et al. Molecular subclasses of high-grade glioma predict prognosis, delineate a pattern of disease progression, and resemble stages in neurogenesis. Cancer cell 2006;9:157–73.
[19] Verhaak RG, Hoadley KA, Purdom E, et al. Integrated genomic analysis identifies clinically relevant subtypes of glioblastoma characterized by abnormalities in PDGFRA, IDH1, EGFR, and NF1. Cancer cell 2010;17:98–110.
[20] Vertosick FTJr, Selker RG. Brain stem and spinal metastases of supratentorial glioblastoma multiforme: a clinical series. Neurosurgery 1990;27:516–21. [discussion 521–512].
[21] Grabb PA, Albright AL, Pang D. Dissemination of supratentorial malignant gliomas via the cerebrospinal fluid in children. Neurosurgery 1992;30:64–71.
[22] Lawton CD, Nagasawa DT, Yang I, et al. Leptomeningeal spinal metastases from glioblastoma multiforme: treatment and management of an uncommon manifestation of disease. J Neurosurg Spine 2012;17: 438–48.
[23] Elliott JP, Keles GE, Waite M, et al. Ventricular entry during resection of malignant gliomas: effect on intracranial cerebrospinal fluid tumor dissemination. J Neurosurg 1994;80:834–9.
[24] Korshunov A, Sycheva R, Golanov A, et al. Gains at the 1p36 chromosomal region are associated with symptomatic leptomeningeal dissemination of supratentorial glioblastomas. Am J Clin Pathol 2007;127:585–90.
[25] Kato H, Fujimura M, Kumabe T, et al. PTEN gene mutation and high MIB-1 labeling index may contribute to dissemination in patients with glioblastoma. J Clin Neurosci 2004;11:37–41.
[26] Shu YJ, Weng H, Ye YY, et al. SPOCK1 as a potential cancer prognostic marker promotes the proliferation and metastasis of gallbladder cancer cells by activating the PI3K/AKT pathway. Molecular cancer 2015; 14:12.
[27] Miao L, Wang Y, Xia H, et al. SPOCK1 is a novel transforming growth factor-beta target gene that regulates lung cancer cell epithelial–-mesenchymal transition. Biochem Biophys Res Commun 2013;440: 792–7.
[28] Li Y, Chen L, Chan TH, et al. SPOCK1 is regulated by CHD1L and blocks apoptosis and promotes HCC cell invasiveness and metastasis in mice. Gastroenterology 2013;144:179–91.e4.
[29] Yang X, Ren H, Yao L, et al. Role of EHD2 in migration and invasion of human breast cancer cells. Tumour Biol 2015;36: 3717–26.
[30] Liu S, Wang J, Guo C, et al. Annexin A11 knockdown inhibits in vitro proliferation and enhances survival of Hca-F cell via Akt2/FoxO1 pathway and MMP-9 expression. Biomed Pharmacother 2015;70: 58–63.
[31] Starska K, Forma E, Jozwiak P, et al. Gene and protein expression of glucose transporter 1 and glucose transporter 3 in human laryngeal cancer—the relationship with regulatory hypoxia-inducible factor-1alpha expression, tumor invasiveness, and patient prognosis. Tumour Biol 2015;36:2309–21.
[32] Wang J, Guo C, Liu S, et al. Annexin A11 in disease. Clin Chim Acta 2014;431:164–8.
[33] Liu YF, Yang A, Liu W, et al. NME2 reduces proliferation, migration and invasion of gastric cancer cells to limit metastasis. PLoS One 2015;10: e0115968.